Available online at www.CivileJournal.org

Civil Engineering Journal

(E-ISSN: 2476-3055; ISSN: 2676-6957)

Vol. 11, No. 08, August, 2025

Natural Frequency of Liquefaction Potential Based on Soil Investigation and Microtremor Observation Results

Rusnardi Rahmat Putra [1*], Junji Kiyono [2], Zhenghu Zhang [3], Sai Vanapalli [4], M. Darma Agung [1]

[1] *Department of Civil Engineering, Universitas Negeri Padang, Sumatera Barat 25131, Indonesia.*

[2] *Department of Urban Management, Graduate School, Kyoto University, Kyoto, 615-8246, Japan.*

[3] *State Key Laboratory of the Coastal and Offshore Engineering, Dalian University of Technology, Dalian, 116024, China.*

[4] *Department of Civil Engineering, University of Ottawa, Ottawa, ON K1N 6N5, Canada.*

Received 19 November 2024; Revised 17 June 2025; Accepted 25 June 2025; Published 01 August 2025

Abstract

This study aims to identify the natural frequency threshold for liquefaction potential by comparing four assessment methods at 54 identical sites in Padang, Indonesia. Methods include: (1) safety factor calculations from soil investigation results (CPT and SPT) applying the 2009 Padang earthquake's peak ground acceleration as input for cycling stress ratio; (2) natural frequency measurements at the surface using microtremor single observations; (3) liquefaction potential assessment through vulnerability index; and (4) analysis of historical liquefaction events from the September 30, 2009 Padang earthquake documented in two previous research papers. The analysis focused on soil depths ranging from 1-4 m. Findings reveal that sites with natural frequencies exceeding 0.40 Hertz remain safe from liquefaction, while sites with frequencies between 0.20-0.39 Hertz demonstrate significant liquefaction potential. This research contributes to the field by establishing a clear correlation between measurable natural frequency thresholds and liquefaction risk, providing engineers and urban planners with a more accessible parameter for preliminary risk assessment. Integrating multiple assessment methods at identical sites enhances the reliability of the identified frequency thresholds, offering a more comprehensive approach to liquefaction hazard mitigation in earthquake-prone regions.

Keywords: Microtremor Single; Natural Frequency; Ground Investigation; Ground Motion; Liquefaction; Innovation and Infrastructure.

1. Introduction

Seasonal earthquakes can cause a lot of damage to human victims as well as damage to public infrastructure. For example, the earthquake that struck off the coast of Sumatra, approximately 50 km northwest of Padang City at a depth of 71 km on September 30, 2009, caused extensive damage to infrastructure, including government buildings, residential areas, roads, irrigation systems, and communication networks. The earthquake had a 7.6 magnitude and caused 1,195 casualties and a loss of 4.8 trillion rupiahs in terms of property [1, 2]. Liquefaction at several locations in Padang further exacerbated the damage [3, 4]. The liquefaction that occurred at various locations in Padang following the September 30, 2009, earthquake was confirmed by the appearance of soil and water being expelled to the surface immediately after the event [5, 6]. Liquefaction was identified in densely populated regions, especially near rivers and swamps. Figures 1(a) and 1(b) illustrate the impacted areas in 2009, which resemble those shown in Figures 1 and 2. This phenomenon

* Corresponding author: rusnardi.rahmat@ft.unp.ac.id

http://dx.doi.org/10.28991/CEJ-2025-011-08-02

© 2025 by the authors. Licensee C.E.J, Tehran, Iran. This article is an open access article distributed under the terms and conditions of the Creative Commons Attribution (CC-BY) license (http://creativecommons.org/licenses/by/4.0/).

is generally triggered by changes in soil conditions, shifting from a drained to an undrained state, which causes an increase in pore pressure, exceeding the effective soil stress [7]. Liquefaction occurs when earthquake-induced cyclic loading reduces or eliminates the effective stress within the soil, leading to a loss of soil strength and stability [8, 9].

Cyclic loading transfers stress from the soil pores to cause effective soil stress; this typically occurs in loose, water-saturated sandy soils [10, 11]. Consequently, the soil is unable to support the load, leading to deformation. The reduction in shear resistance happens because pore stresses are directly transferred to the effective stresses between the soil particles. The stress within the pores swiftly increases, while the effective stress between the soil particles remains unchanged [12, 13]. In severe cases, the effective stress may reach zero, meaning the soil particles are no longer statically bound together. Liquefaction during an earthquake can be recognized by horizontal ground movement, water seeping from soil fractures, building tilting or sinking, land subsidence, and landslides affecting embankments and slopes [14]. The liquefaction potential of sandy soils is influenced by the relative density and effective stress parameters [15, 16]. Buildings in liquefied areas can collapse, tilt, shift sideways, or even be completely destroyed [17].

Liquefaction primarily occurs in semi-impermeable sandy soils, including silty sand, clayey sand, and fine sand. This phenomenon arises because these soils possess large pores or cavities, making it challenging to reach maximum density [18]. Soils with larger pores exhibit good porosity, forming a saturated water condition [19].

Despite extensive research on liquefaction phenomena, a significant gap exists in establishing reliable correlations between measurable field parameters and liquefaction potential across different geological settings. Previous studies have primarily focused on either geotechnical investigations [20, 21] or seismic response analyses [22, 23], with limited integration between these approaches. This study addresses this research gap by comprehensively integrating four distinct methods—safety factor calculations from soil investigations, natural frequency measurements from microtremor observations, vulnerability index assessments, and historical liquefaction event analyses—at 54 identical sites in Padang. By correlating natural frequency thresholds with liquefaction potential, this research aims to develop a more accessible parameter for preliminary risk assessment that can be efficiently deployed in earthquake-prone regions with similar geological characteristics.

1.1. Geological Conditions and Liquefaction Event Due to Padang Earthquake on September 30 2009

Padang, the capital of West Sumatra province, has a high population density and is located at coordinates 100.38°E, 0.95°S. Geological studies indicate that the soil in Padang primarily consists of sediments, including coastal embankment deposits, hardened crystal tufa, and river sediment (Figure 1) [24, 25].

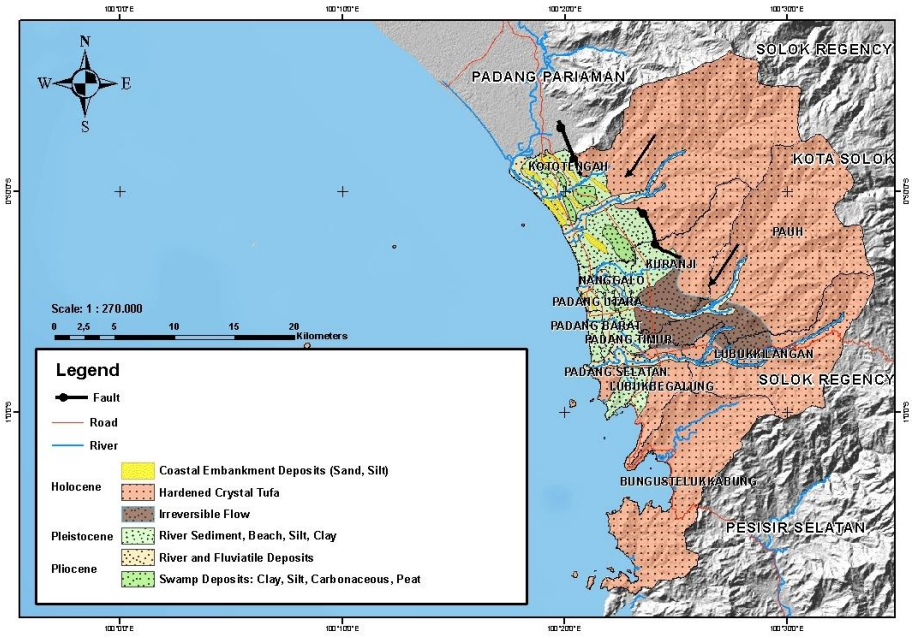

Figure 1. Geological Map of Padang City

The coastal geological profile is characterised by loose sand deposits and gravel, interspersed with discontinuous layers of silt and clay. The distribution of the northwestern coastal embankment is more prominent and serves as the primary source zone for these deposits [19]. Saturated soils with loose sandy structures are prone to liquefaction. Furthermore, the groundwater level in Padang is shallow, ranging from 2.00 to 4.89 m, facilitating easy water saturation [26]. The potential for liquefaction in soil is influenced by the density of the sand layer, which increases with depth.

Additionally, the shallow groundwater level exacerbates the impact of earthquakes [27]. For liquefiable layers like sand-clay composites, the effect of frequency within the 5–30 Hz range shows that an increase in vibration frequency leads to a reduction in the liquefaction area and surface subsidence [28].

Padang is the capital city of West Sumatra Province and is located on the west coast of Sumatra Island in Indonesia. The region experienced significant seismic activity, with over 1000 casualties reported from the M 7.6 earthquake on September 30, 2009. Additionally, a seismic gap has been identified offshore from Padang, at the boundary between the Eurasian and Indo-Australian plates, where an M 8.0 earthquake is anticipated [29]. The M 7.6 earthquake on September 30, 2009, led to liquefaction incidents in various parts of Padang, as illustrated in Figure 2.

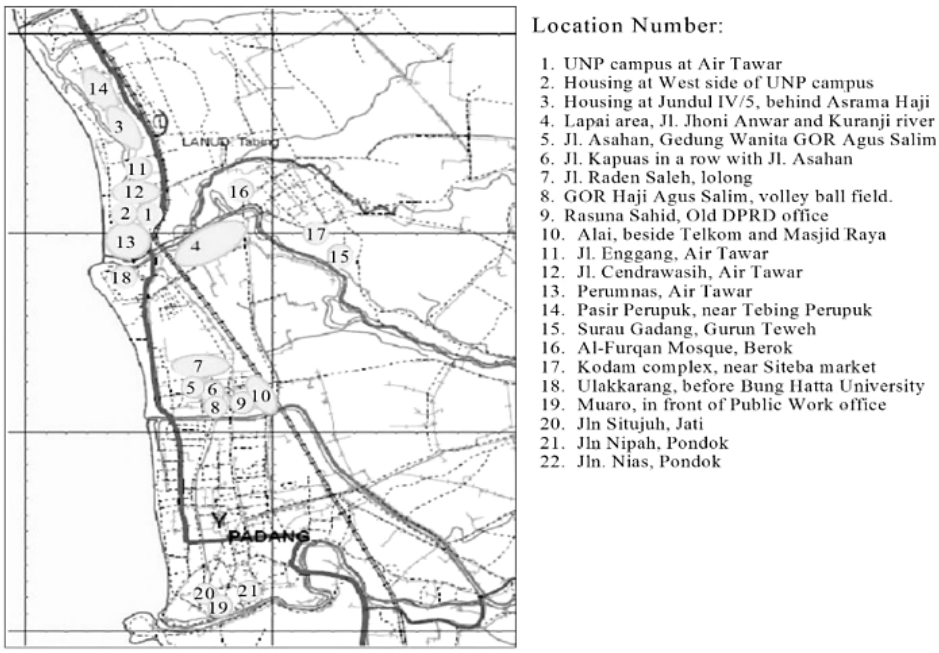

(a)

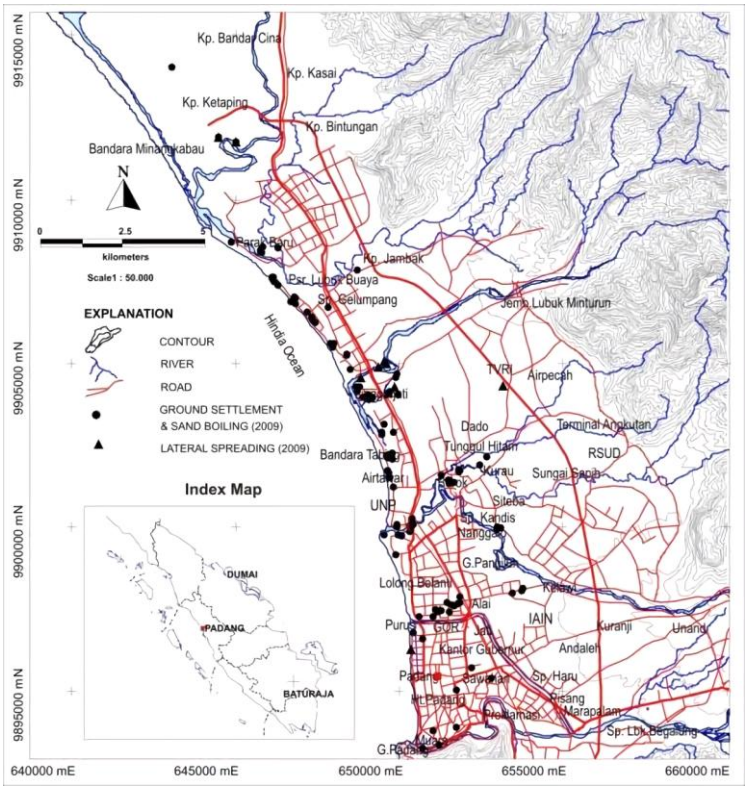

(b)

Figure 2. Map representations of liquefaction events caused by the September 30, 2009, Padang earthquake, including (a) a liquefaction map produced by Hakam et al. [5] and (b) another liquefaction map created by Tohari et al. [6]

Padang comprises 11 districts, covering a total area of 694.96 km². The largest district is Koto Tangah, which spans 232.25 km², accounting for one-third of the city's total area, while the smallest is West Padang District, measuring just seven km². According to the 2020 population census, Padang City has a population of 973,152 people [30]. The Koto Tangah District is the most populated, with 203,842 residents, whereas the Teluk Bungus District has the smallest population, totalling 25,867 people. The average population density for Padang City in 2020 was 1370 people/km² [30]. These maps highlight the geographical spread of liquefaction occurrences due to the seismic event, offering insights into how the earthquake-induced liquefaction impacted different areas in Padang.

2. Research Methodology

2.1. Materials

This research was conducted in Padang, encompassing 54 observation sites. At each site, tests to assess soil resistance were performed using data from soil investigations, which included the Cone Penetration Test (CPT) and the Standard Penetration Test (SPT). Additionally, single microtremor observations were carried out, and liquefaction events related to the 2009 earthquake were examined. These tests aimed to understand the soil's behaviour under seismic conditions and its susceptibility to liquefaction following the quake.

2.2. Methods

In determining the liquefaction potential for each site (soil investigation), a deterministic method of analysis, based on the formulation by Seed & Idriss (1971) [21], involves comparing the Cyclic Resistance Ratio (CRR), which represents the soil's ability to resist deformation, with the Cyclic Stress Ratio (CSR), which characterises the earthquake-induced stress on the soil. When using the simplified method to estimate the shear stresses generated in the soil due to seismic loading, the CSR at any given depth (1-4 m below the surface) is calculated using the maximum ground acceleration recorded over the past 500 years. This calculation provides insight into the soil's vulnerability to liquefaction during seismic events by evaluating how much stress it can handle before failure.

The study also performed single microtremor observations at the same 54 sites where the SPT and CPT tests were conducted (Figure 3). These microtremor measurements aim to determine the natural frequency of the soil by analysing the Horizontal to Vertical Spectral Ratio (HVSR). The result of the microtremor measurement is the natural frequency parameter (f_o), which helps to identify the relationship between the soil's natural frequency and its liquefaction potential. Researchers can better assess soil's susceptibility to liquefaction during seismic activity by correlating natural frequencies with liquefaction risk.

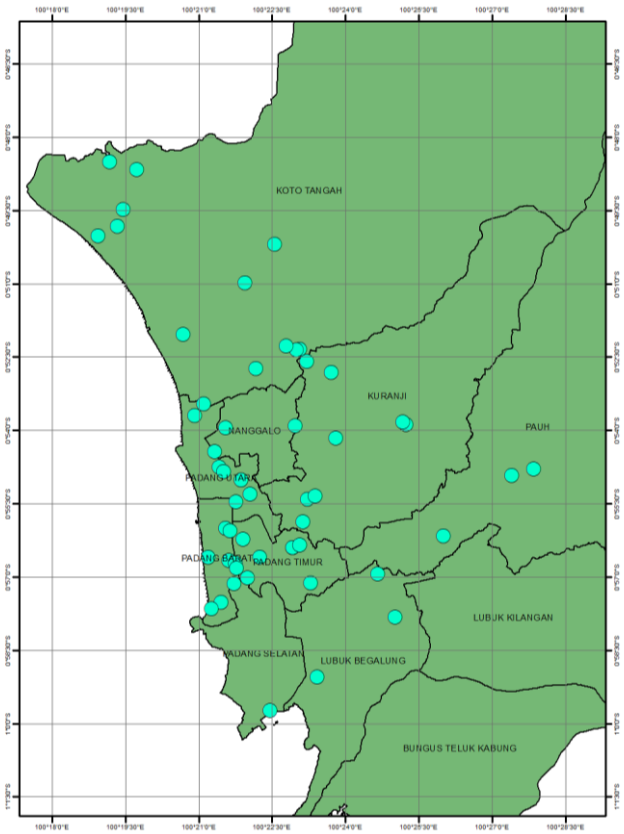

Figure 3. Research Locations, Padang city, Indonesia

The resistance criteria used to evaluate liquefaction potential at a site generally provide consistent outcomes, regardless of the method employed. Both SPTs (Standard Penetration Tests) and CPTs (Cone Penetration Tests) are recommended due to their extensive database and proven effectiveness through years of application [31]. However, alternative methods may be more practical at locations where there are gravel sediments or difficult road access. For such challenging sites, the methods proposed by Youd & Idriss [32] offer alternative approaches for assessing liquefaction potential. Other researchers, like Sonmez & Gokceoglu [33], have also explored alternative techniques that can be applied in challenging terrain, providing flexibility in liquefaction assessments under varied site conditions. This collective research confirms the adaptability of these methods, ensuring accurate evaluations of liquefaction risk across different types of sites.

2.3. Liquefaction Potential Evaluation Based on Soil Investigation Results

2.3.1. The Normalisation of Soil Stress

The cyclic stress ratio (CSR) is a critical indicator in evaluating the potential for soil liquefaction during seismic events. It reflects the normalised stress exerted on soil layers, influenced by the total overburden pressure. Notably, CSR values tend to diminish in the upper layers while escalating in deeper layers, often resulting in liquefaction phenomena commencing in the surface soils. In this investigation, we conducted soil assessments at 1 m intervals, with a maximum depth of 7m, to capture the variations in CSR based on the groundwater level at the target site. The CSR calculation using the method proposed by Seed & Idriss (1971) [21] is:

$$\sigma_{cyc} = 0.65 \frac{\alpha_{max}\sigma}{g\,\sigma'_v} r_d \quad (1)$$

In this context, α_{max} represents the peak ground surface acceleration, g denotes the acceleration due to gravity at depth z, σ is the total stress at depth z, σ'_v is the effective vertical stress at depth z and "r_d" is a correction factor accounting for the soil depth. The cyclic stress generated by the earthquake is estimated using the simplified method proposed by Seed & Idriss (1971) [21].

The maximum ground acceleration value is derived from the ground motion data recorded during the September 30, 2009, Padang earthquake. The peak ground acceleration (PGA) recorded was 0.38 g (see Figure 4), associated with a magnitude of Mw 7.6. This PGA value aligns with the observed liquefaction related to the Padang earthquake on September 30, 2009, as discussed in studies by Hakam et al. [5] & Tohari et al. [6].

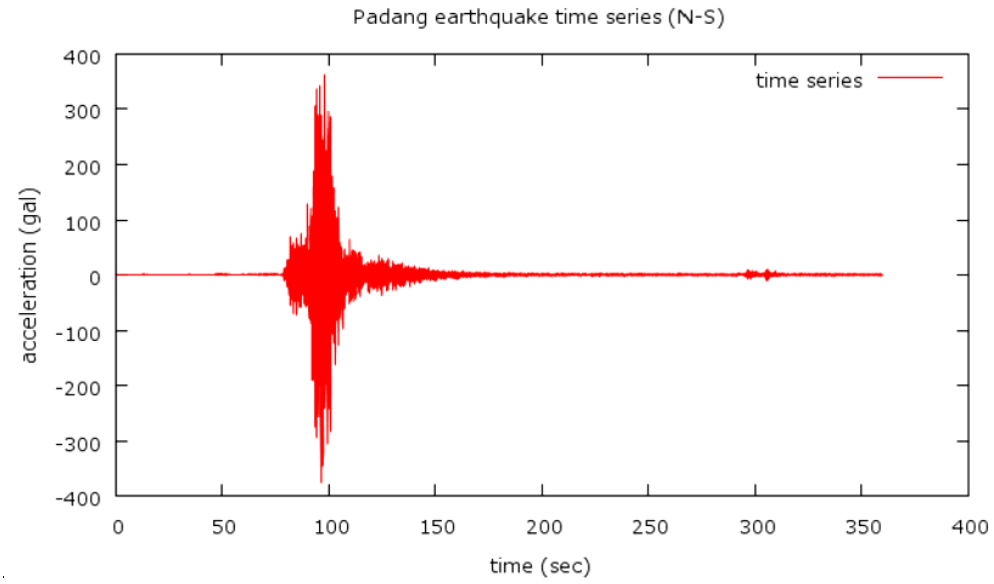

Figure 4. Padang earthquake ground motion record N-S direction

2.3.2. Cyclic Resistance Ratio (CRR) Value in Each Soil Layer

The CRR value method varies for each set of CPT and SPT data [34]. For CPT data, an empirical equation is provided by Robertson & Wride [34] to derive the CRR value based on the corrected cone penetration qc_1, expressed as follows:

$$CRR_m = 0.833\,(q_{c1}/1000)^3 + 0.05 \quad ;\ q_{c1} < 50 \quad (2)$$

$$CRR_m = 93 \times (q_{c1}/1000)^3 + 0.08 \quad ;\ 50 < q_{c1} < 160 \quad (3)$$

For SPT data, the CRR value is calculated using the following equation:

$$CRR_m = \frac{1}{34-(N_1)_{60}} + \frac{(N_1)_{60}}{135} + \frac{50}{[10-(N_1)_{60}+45]^2} - \frac{1}{200} \quad (4)$$

where $(N_1)_{60}$ represents the number of corrected SPT blows and corresponds to an overburden pressure approximately 100 kPa, with an energy efficiency of 60% for the blows (Table 1). The value of $(N_1)_{60}$ is calculated using the following equation:

$$(N_1)_{60} = N_m C_N C_E C_B C_R C_S \quad (5)$$

Table 1. Correction factors in the SPT test

Factors	Tools Variable	Symbols	Correction
Overburden pressure	-	C_N	$(P/\sigma'_{v0})^{0.5}$
Overburden pressure	-	C_N	$C_N \leq 1.7$
Energy ratio	Donut hammer	C_E	0.5 – 1.0
Energy ratio	Safety hammer	C_E	0.7 – 1.2
Energy ratio	Automatic – trip donut – type hammer	C_E	0.8 – 1.3
Hole diameter (drill size)	65 – 115 mm	C_B	1.00
Hole diameter (drill size)	150 mm	C_B	1.05
Hole diameter (drill size)	200 mm	C_B	1.15
Rod length	< 3 m	C_R	0.75
Rod length	3 – 4 m	C_R	0.80
Rod length	4 – 6 m	C_R	0.85
Rod length	6 – 10 m	C_R	0.95
Rod length	10 – 30 m	C_R	1.00
Sampling method	Standard	C_S	1.00
Sampling method	Unlimited sampling	C_S	1.1 – 1.3

2.3.3. Safety Factor (SF)

The safety factor (SF) is a key metric used to assess the liquefaction potential of a given site. It is calculated by comparing the cyclic resistance ratio (CRR) to the cyclic stress ratio (CSR). If the SF value is less than 1.0, the soil is susceptible to liquefaction, whereas a value greater than 1.0 indicates that the soil is safe from liquefaction. The following equation can express the SF:

$$SF = (CRR/CSR)MSF \quad (7)$$

where MSF represents the Magnitude Scaling Factor, as defined by Seed & Idriss (1971) [21]. The MSF value is calculated using the following equation:

$$MSF = \frac{10^{2.24}}{M_w{}^{2.56}} \quad (8)$$

where *Mw* is the magnitude of the earthquake.

Table 1 shows the correction values for the $N_{1(60)}$ calculations.

2.3.4. Microtremor Measurements

Microtremor measurements were conducted at the locations where the CPT and SPT data were collected. Seismic waves were captured using a GPL-6A3P microtremor sensor, and the data were analysed using the Horizontal to Vertical Spectral Ratio (HVSR) method, as Nakamura [35] and Nakamura [36] outlined. This method examines the spectral ratio between the horizontal (H) and vertical (V) components of the Fourier amplitude spectra of the recorded seismic waves. The peak period of the HVSR corresponds to the resonance period of the soil under investigation. Both horizontal components (NS and EW) and the vertical component (UD) were recorded simultaneously for 10 minutes, with a sampling frequency of 100 Hz, following the guidelines from the Site Effects Assessment Using Ambient Excitations [37, 38].

A key result from the microtremor measurements at a given site is the dominant frequency (f_0) obtained from the HVSR graph. Processing microtremor data using the spectral ratio method is widely regarded as one of the most reliable and straightforward techniques for determining the dynamic characteristics of soils and structures, mainly the

predominant frequency. Nakamura [35] pioneered this method, highlighting its simplicity and effectiveness in identifying site resonance. Later, Bonnefoy-Claudet et al. [39] reinforced its reliability, emphasising its ability to provide accurate estimates of soil characteristics with minimal equipment. Similarly, the SESAME [40] acknowledged the HVSR method as a standard approach for site effect studies, given its practical application in seismic risk assessment and structural analysis. Precise peak frequencies from the HVSR curves, derived from the microtremor recordings, are illustrated in Figures 5-a and 5-b.

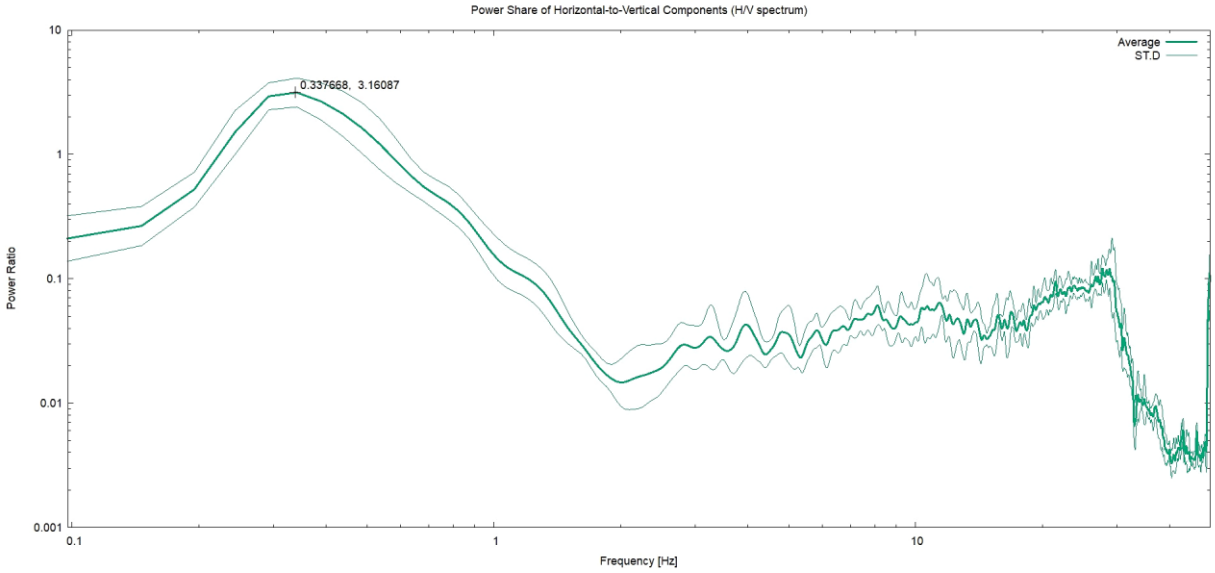

(a)

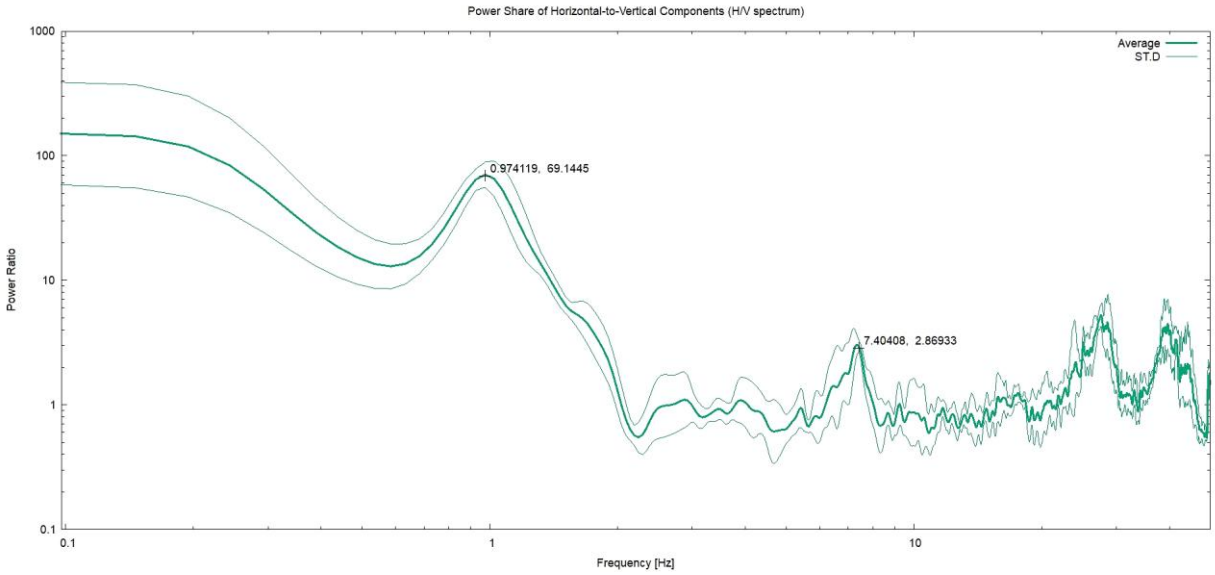

(b)

Figure 5. Clear Peak of HVRs, located (a) Kampus UNP (b) Kuranji

The natural frequency of soil is affected by both the thickness of the weathered layer (H) and the shear wave velocity (V_s) [41]. Typically, locations with thicker sediment layers exhibit lower natural frequency values, as noted by Karagianni et al. [42] and supported by other studies (e.g. [43, 44]). These findings emphasise the relationship between sediment thickness and natural frequency in various geological contexts. Figure 6 provides an overview of the microtremor device employed and the field observations made during the measurements. The flow chart in Figure 7 shows the procedure followed.

$$HVSR = \sqrt{\frac{F_{NSi}(\omega)^2 + F_{FWi}(\omega)^2}{F_{UDi}(\omega)^2}} \quad (9)$$

$F_{NSi}(\omega)$ and $F_{UDi}(\omega)$represent the Fourier amplitudes of the North-South (NS) and East-West (EW) components, respectively, while UD refers to the vertical element for each interval, and ω denotes the frequency.

Figure 6. Microtremor GPL-6A3P Sensor (left), field survey (right)

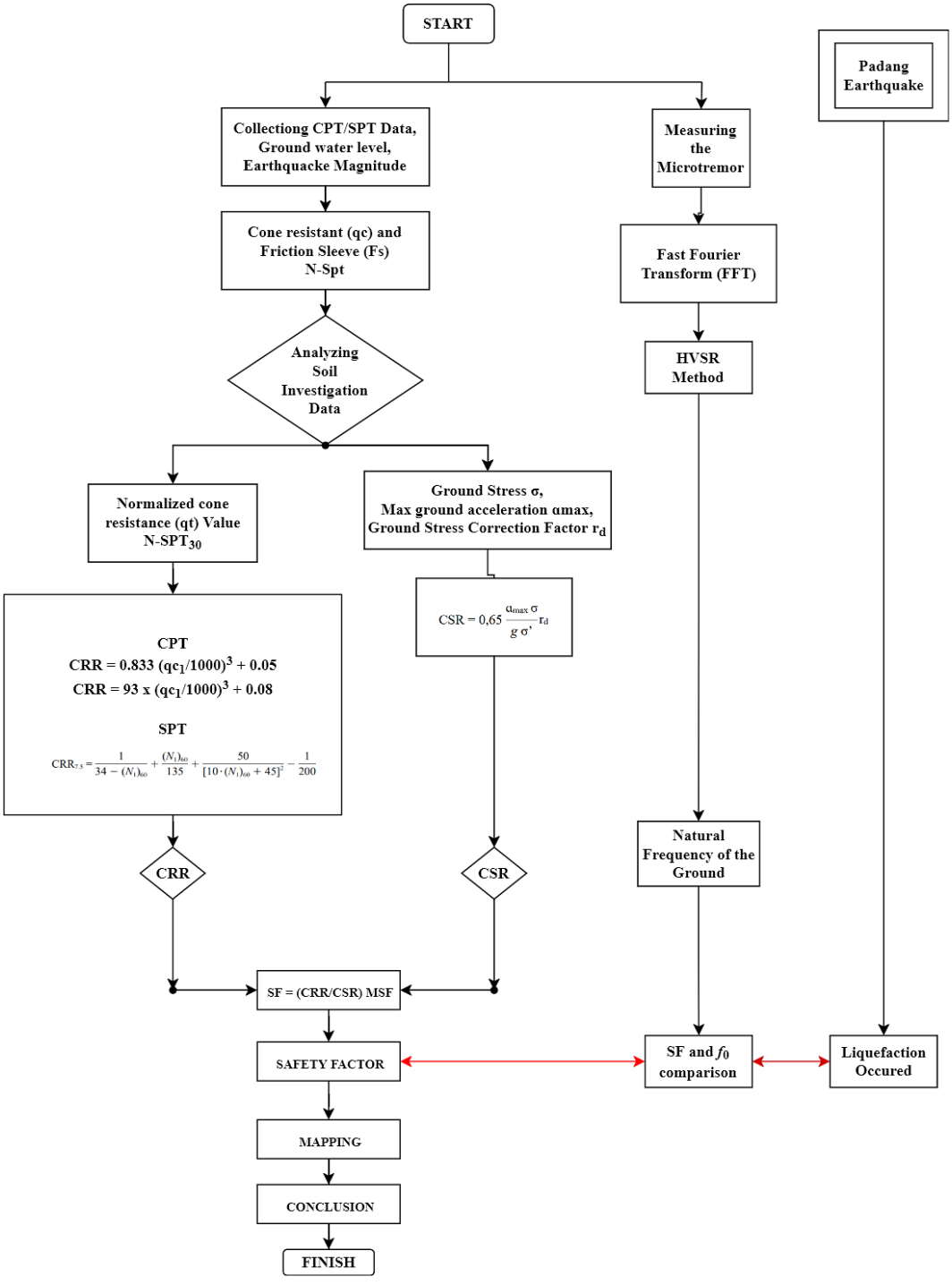

Figure 7. Research Flow Chart

The HVSR analysis of the microtremor data was conducted by the guidelines established by Nakamura [45], to ensure the accuracy of the results and to identify precise peak frequencies. Figure 5 presents examples of the distinct peak frequency HVSR curves derived from the microtremor recordings. Noisy windows, including transient and stationary near-white noise, were excluded from the analysis to enhance the quality of the results.

2.3.5. Liquefaction Potential by Using Microtremor Observation Results

Earthquakes influence soil stability depending on the soil's characteristics and properties. Liquefaction can occur when effective ground stress is reduced due to cyclic loading from seismic shaking [8]. During cyclic loading, pore pressures increase, which affects the effective ground stress, particularly in saturated, loose, sandy soils. As a result, the soil may be unable to support loads, leading to deformation [20, 46]. When determining the liquefaction potential, higher Kg values indicate that damage is more likely [35]. The Kg value only comes from the strain of the soil structure. According to Choobbasti et al. [47], liquefaction can occur if the Kg value exceeds 5.0. This threshold can be defined as follows:

$$K_g = \frac{A^2}{f_0} > 5 \quad (10)$$

where the K_g is the vulnerability index, A is the amplification from the HVSR result, and f_0 is the natural frequency of the subsoil structure.

3. Results and Discussion

3.1. Liquefaction Risk Assessment Using Soil Investigation Findings

Using ground investigation data from 54 analysed points, we determined the cyclic resistance ratio (CRR) and cyclic stress ratio (CSR) values at depths ranging from 1-4 m. The CRR values ranged from 0.493 to 2.125, while the CSR values ranged from 0.3160 to 1.0485. These values are crucial for evaluating the potential for soil liquefaction during seismic events. Figure 8 compares CRR and CSR values at various locations within the study area, specifically at T1, T2, T14, and T38, which were selected based on their groundwater levels.

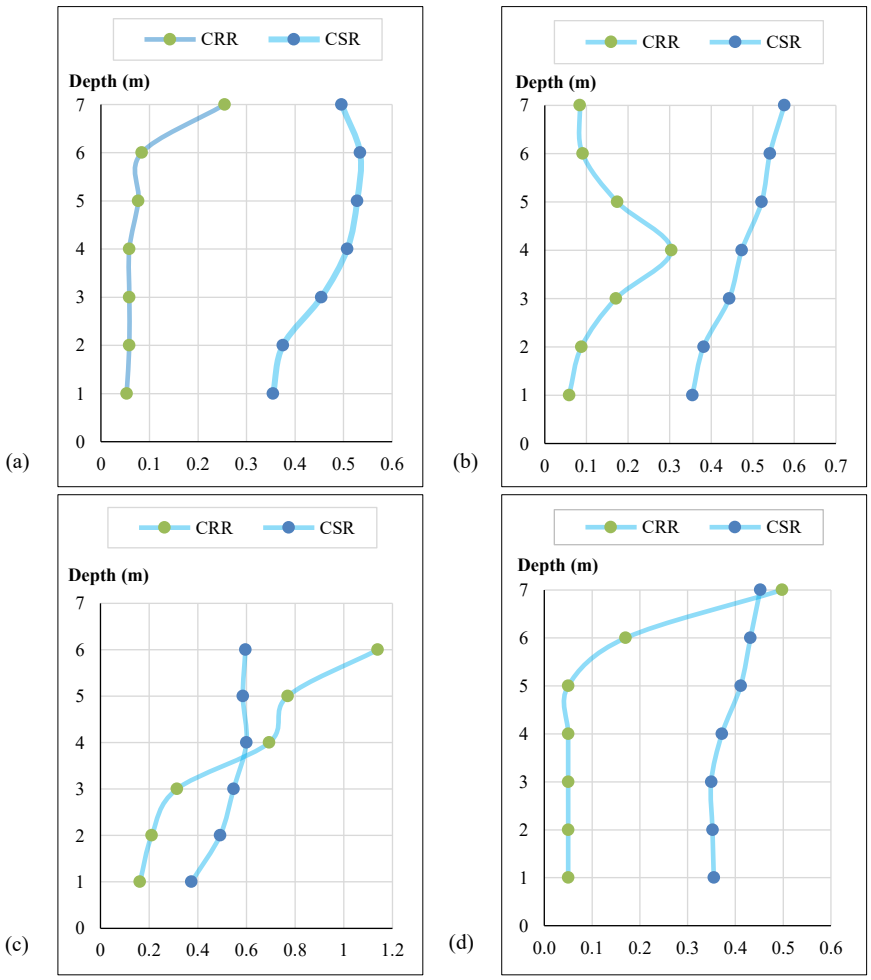

Figure 8. CRR and CSR Values at Several Points: (a) T1 (Air Pacah), (b) T2 (Gedung Walikota), (c) T14 (Koto Tangah) and (d) T38 (Teluk Bayur)

By comparing the CRR values with the CSR values, we can establish the safety factor against liquefaction. A safety factor below 1.0 indicates a heightened risk of liquefaction, while values above 1.0 suggest that the soil is likely to remain stable. Additionally, to visually represent the area's susceptibility to liquefaction, we mapped this potential using kriging, a spatial interpolation method that estimates values across a continuous surface.

As depicted in Figure 9, this mapping categorises areas into different risk levels: dark red indicates extreme potential for liquefaction, red signifies high potential, bright red represents potential, orange indicates moderate potential, yellow reflects low potential, and green shows no potential for liquefaction. This classification helps understand and mitigate risks associated with seismic activity in the area.

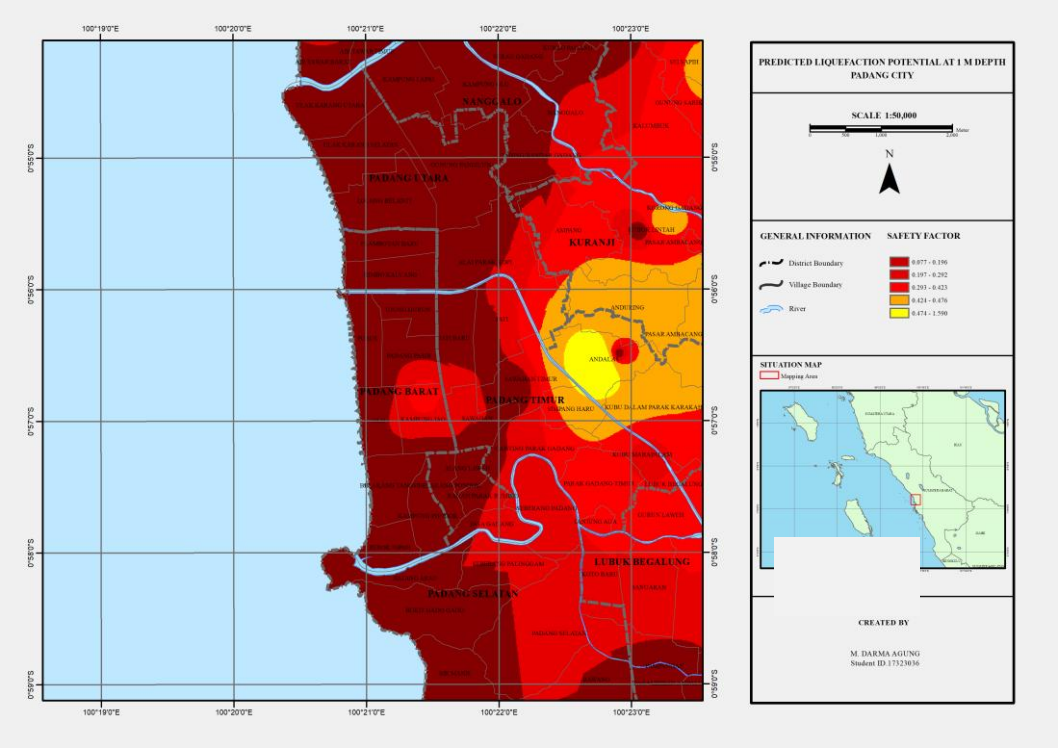

(a)

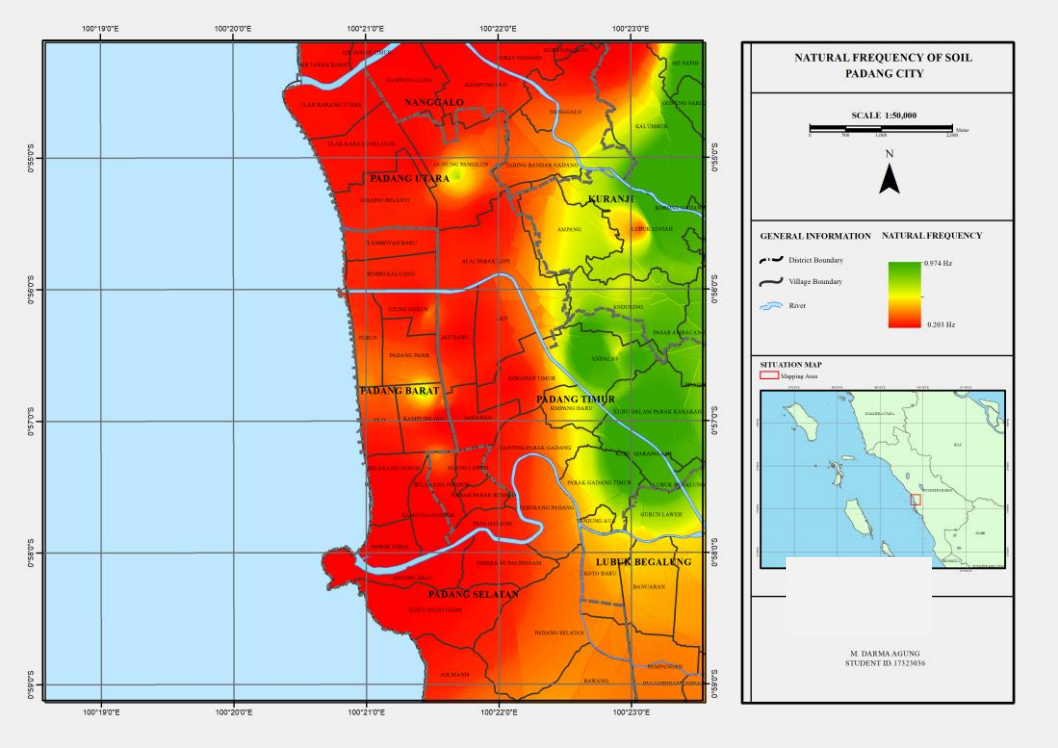

(b)

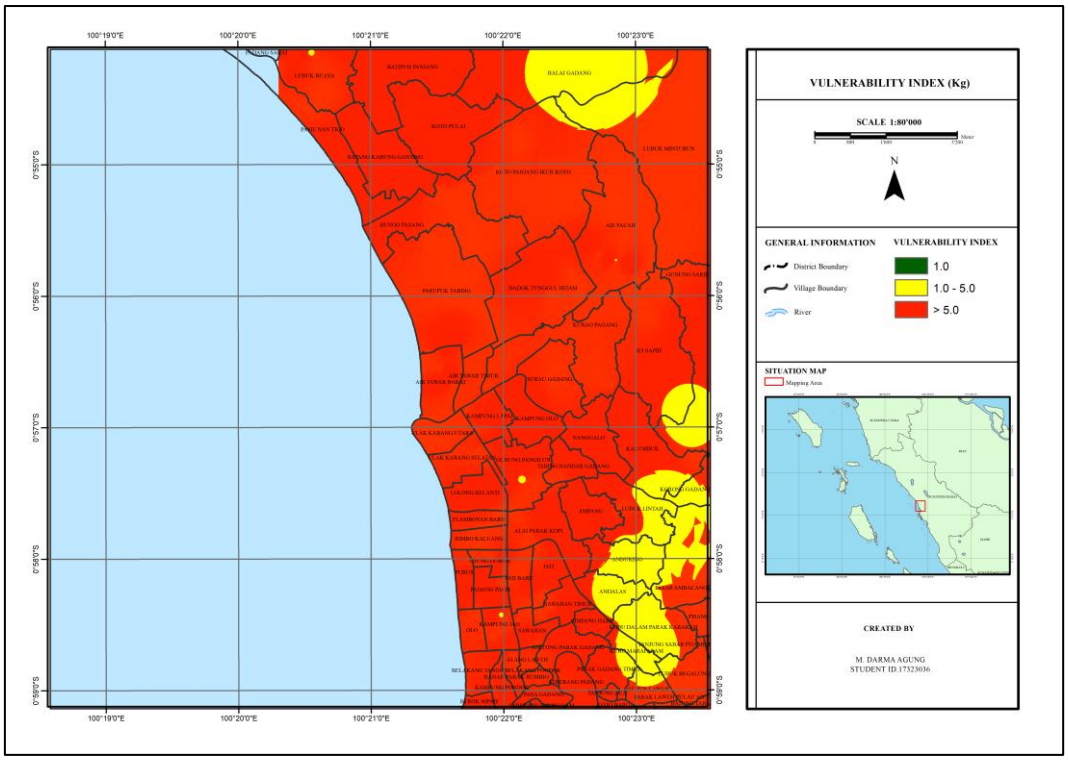

(c)

Figure 9. Map of liquefaction potential and predominant frequency: (a) liquefaction risk at depths ranging from 1-4 m; (b) predominant frequency of soil; and (c) liquefaction potential based on vulnerability index, Kg ≥ 5

3.2. Natural Frequency of Soil

The natural frequency f_o in the study area ranges from 0.202 to 0.974 Hz, with an average value of 0.358 Hz. This frequency suggests that the soil surface at the study site is primarily composed of alluvial deposits formed from sedimentation, soft soils, and mud, with a layer thickness reaching up to 30 m (Vs_{30}). This conclusion is further supported by SPT data from several test points, which classify the soil as sandy loam (SC) and coarse sand (SP) to a depth of 30 m. Notably, the highest f_o was recorded at point 43 (Belimbing, Kuranji), while the lowest value was observed at point 49. These variations in frequency reflect the heterogeneous nature of the subsurface materials in the area.

By examining the relationship between the soil's natural frequency and the liquefaction potential at the test points, alongside the liquefaction events triggered by the Padang earthquake in 2009, we can evaluate the liquefaction vulnerability index. The results are summarised in Table 2 and illustrated in Figures 10-a, 10-b, and 10-c. Points deemed safe from liquefaction exhibit a natural frequency greater than 0.40 Hz, while those with liquefaction potential fall within 0.20-0.39 Hz range. There is no potential for liquefaction due to the more significant value; dense and solid soils are more resistant to cyclic loads. The opposite result occurred at sites 12 (0.29 Hz) and 49 (0.1418 Hz). i.e. 'Not Potential' (1.8% from the data obtained from soil investigation, CPT and SPT, and the liquefaction potential from vulnerability index, respectively. The good agreement between liquefaction potential where the vulnerability index is greater than 5 [38] and the proposed result in this study with a range within 0.20-0.39 Hz.

Table 2. Liquefaction field survey, SPT-borehole and microtremor single observation result

	Hakam et al. [5]	Tohari et al. [6]	Safety Factor	Conclusion	Frequency (Hz)	Periods (s)	Soil Type	Amplitude	Vulnerability Index (K_g) value of liquefaction potential is $K_g \geq 5$. $Kg = A^2 / f$	Conclusion
T1	P	P	0.1508	P	0.2935	3.4071	Soft	3.40716	39.5527	P
T2	P	P	0.2233	P	0.2031	4.9236	Soft	3.30142	35.9834	P
T3	P	P	0.1376	P	0.3029	3.3014	Soft	2.574	17.0540	P
T4	P	P	0.1142	P	0.3885	2.5740	Soft	2.94118	25.4427	P
T5	P	P	0.1373	P	0.3400	2.9411	Soft	2.92056	24.9114	P
T6	P	P	0.1111	P	0.3424	2.9205	Soft	2.94118	25.4427	P

T7	P	P	0.1373	P	0.3400	2.9411	Soft	2.96121	25.9661	P
T9	P	P	0.2311	P	0.2937	3.4048	Soft	3.40483	39.4719	P
T10	P	P	0.2866	P	0.3898	2.5654	Soft	2.56542	16.8840	P
T11	P	P	0.0906	P	0.2917	3.4281	Soft	3.42818	40.2894	P
T12	P	P	0.2019	P	0.3895	2.5673	Soft	2.56739	16.9230	P
T13	NP	NP	3.4111	NP	0.2907	3.4399	Soft	3.43997	40.7066	P
T14	P	P	0.4142	P	0.3412	2.9308	Soft	2.93083	25.1752	P
T15	P	P	0.0912	P	0.2915	3.4305	Soft	3.43053	40.3724	P
T16	P	P	0.0875	P	0.3083	3.2435	Soft	3.24359	34.1255	P
T17	P	P	0.0777	P	0.2915	3.4305	Soft	3.43053	40.3724	P
T18	P	P	0.1315	P	0.2925	3.4188	Soft	3.4188	39.9597	P
T19	P	P	0.1768	P	0.2915	3.4305	Soft	3.43053	40.3724	P
T20	P	P	0.7883	P	0.3436	2.9103	Soft	2.91036	24.6513	P
T21	P	P	0.3630	P	0.3912	2.5562	Soft	2.55624	16.7033	P
T22	P	P	3.5335	NP	0.3926	2.5471	Soft	2.54712	16,.5253	P
T23	P	P	0.4111	P	0.3412	2.9308	Soft	2.93083	25.1752	P
T24	P	P	0.0689	P	0.2925	3.4188	Soft	3.4188	39.9597	P
T25	P	P	0.4877	P	0.2429	4.1169	Soft	4.11692	69.7778	P
T26	P	P	0.1362	P	0.2463	4.0600	Soft	4.06009	66.9278	P
T27	P	P	0.0756	P	0.3898	2.5654	Soft	2.56542	16.8840	P
T28	P	P	0.1373	P	0.2904	3.4435	Soft	3.44353	40.8329	P
T29	P	P	0.1373	P	0.3083	3.2435	Soft	3.24359	34.1255	P
T30	P	P	0.1758	P	0.3871	2.5833	Soft	2.58331	17.2397	P
T31	P	P	1.2203	NP	0.3400	2.9411	Soft	2.94118	25.4427	P
T32	NP	NP	3.7500	NP	0.4693	2.1308	Soft	2.13083	9.6749	P
T33	NP	NP	5.2471	NP	0.3898	2.5654	Soft	2.56542	16.8840	P
T34	P	P	0.6439	P	0.3400	2.9411	Soft	2.94118	25.4427	P
T35	P	P	0.1318	P	0.2463	4.0600	Soft	4.06009	66.9278	P
T36	P	P	0.1336	P	0.3871	2.5833	Soft	2.58331	17.2397	P
T37	P	P	0.1181	P	0.3400	2.9411	Soft	2.94118	25.4427	P
T38	P	P	0.1374	P	0.2894	3.4554	Soft	3.45543	41.2576	P
T39	P	P	0.1373	P	0.2463	4.0600	Soft	4.06009	66.9278	P
T40	P	P	0.1296	P	0.2030	4.9261	Soft	4.92611	119.5396	P
T41	P	P	0.0865	P	0.3412	2.9308	Soft	2.93083	25.1752	P
T42	NP	NP	2.2418	NP	0.4693	2.1308	Soft	2.13083	9.6749	P
T43	P	P	0.3185	P	0.3741	1.0265	Soft	1.02659	1.0819	NP
T44	NP	NP	1.7938	NP	0.5270	1.8975	Soft	1.89753	6.8323	P
T45	P	P	0.3493	P	0.3961	2.5246	Soft	2.52461	16.0911	P
T46	P	P	0.6549	P	0.3743	2.1083	Soft	2.10837	9.3722	P
T47	P	P	0.1265	P	0.2927	3.4164	Soft	3.41647	39.8779	P
T48	NP	NP	1.6119	NP	0.6854	1.4590	Soft	1.459	3.1058	NP
T49	P	P	0.1418	P	0.2030	4.9261	Soft	4.92611	119.5396	P
T50	P	P	0.3049	P	0.3436	2.9103	Soft	2.91036	24.6513	P
T51	P	P	0.0974	P	0.3412	2.9308	Soft	2.93083	25.1752	P
T52	P	P	0.0775	P	0.2907	3.4399	Soft	3.43997	40.7066	P
T53	NP	NP	1.2507	NP	0.3961	2.5246	Soft	2.52461	16.0911	P
T54	P	P	0.2225	P	0.2894	3.4554	Soft	3.45543	41.2576	P

Where P is 'Potential' and NP is 'Not Potential'.

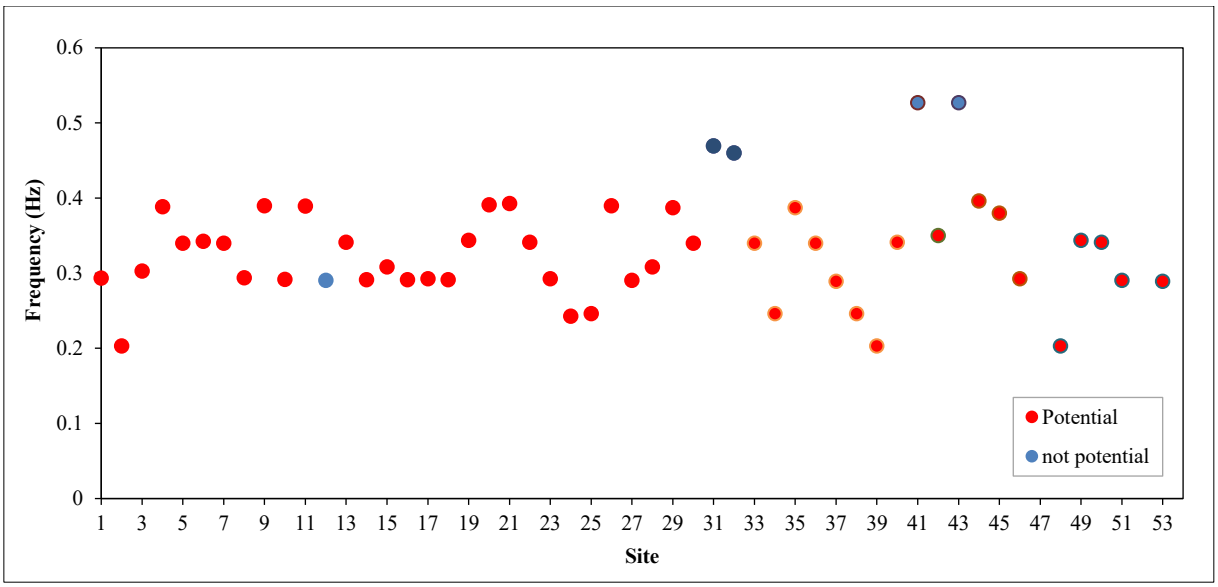

(a)

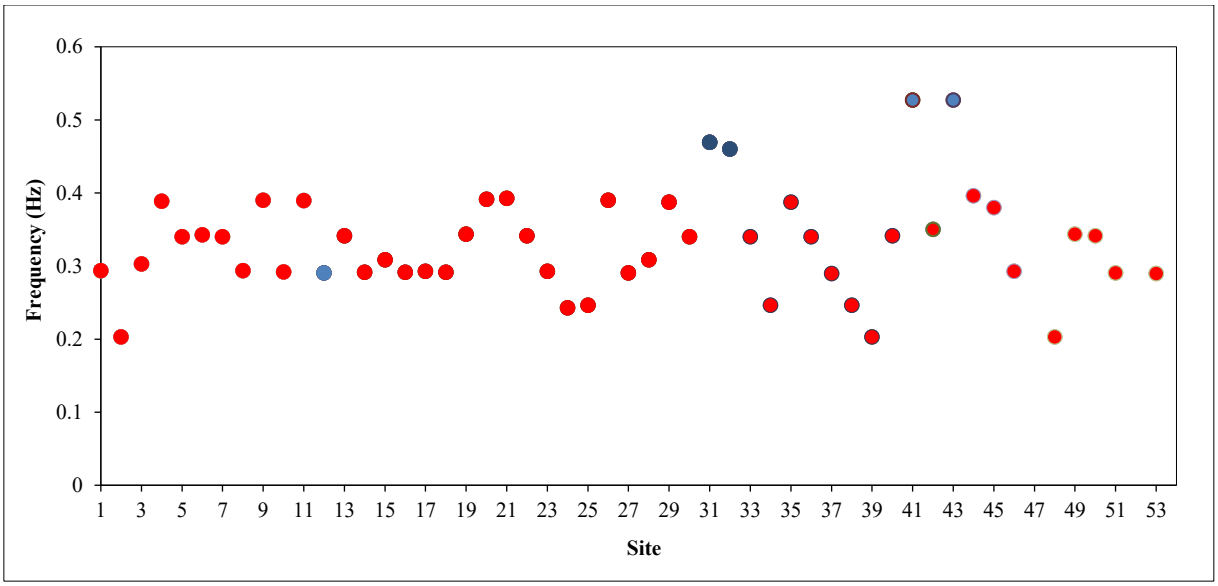

(b)

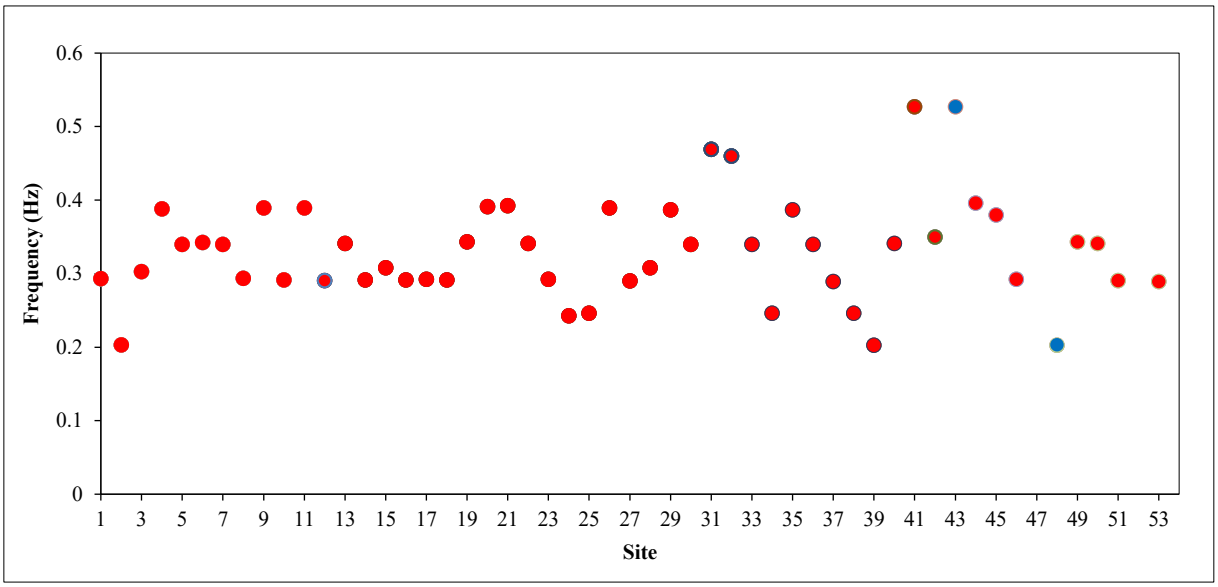

(c)

Figure 10. Comparison of the four methods: (a) natural frequency vs. occurred liquefaction events; (b) natural frequency vs. soil investigation; and (c) natural frequency vs liquefaction potential from vulnerability index

Many aspects produce the liquefaction potential. The most fundamental aspect is on the natural characteristics of the soil layer, and the obvious reduction of the soil rigidity due to significant liquefaction is unique in seismic responses of the site, and it is suitable to take the change of the horizontal natural frequency of the site as a fundamental benchmark for site liquefaction identification [48].

Liquefaction-related damage to civil infrastructure was observed in Palu in 2018, Padang City and Padang Pariaman City in 2009, and Prince William Sound (Alaska) in 1964. The 1964 Prince William Sound earthquake in Alaska was a pivotal event that highlighted the issue of liquefaction and contributed to understanding how to mitigate the risks associated with liquefaction-related disasters. This study proposes a complete procedure to determine the natural frequency range of potential liquefaction by considering existing liquefaction events due to the September 2009 Padang earthquake and the dynamic soil characteristics from SPTs and CPTs, microtremor observations, natural frequency, dynamic characteristics, and liquefaction potential at every liquefaction event. This study focused on a single major earthquake event in Padang on September 30, 2009, with a magnitude of Mw 7.6. This earthquake resulted in 54 instances of liquefaction throughout the city of Padang.

Zhu et al. [49] investigated the impact of cyclic loading on the liquefaction and post-liquefaction resistance of the original sand. Their findings indicated that the excess pore water pressure generation rate increases with higher cyclic loading frequencies, while the cyclic liquefaction resistance decreases as the loading frequency rises. Additionally, research on dynamic properties revealed that the shear modulus decreases and the damping ratio increases with frequency [50] observed a significant decrease in the natural frequency ratio following liquefaction, particularly for offshore conditions with weaker soil, as the depth of liquefaction increases. Furthermore, as the frequency rises from one-hundredth of a Hertz, the damage sustained per loading cycle diminishes while the number of cycles needed to induce liquefaction increases. This finding was corroborated by Chang et al. [51], and further reinforced by subsequent research conducted by Jahankhah & Farashah [52], which emphasized the influence of loading cycles and frequency on the susceptibility to liquefaction.

The main consequence of liquefaction is that it affects the natural characteristics of the upper soil layer, resulting in a marked decrease in soil stiffness. This reduction is particularly evident in the seismic behaviour of the site, which makes the variation in horizontal natural frequency an essential indicator for detecting liquefaction events, as well as research by Mehrzad et al. [53]. The latter also emphasised the significance of changes in natural frequency concerning liquefaction identification.

Comparison of the parameter results from four essential sources (soil investigations using SPT and CPT, the liquefaction investigation due to the 2009 earthquake, seismic behaviour of the soil at the surface during the Padang earthquake, and microtremor single observations for 54 observation sites distributed across all of the liquefaction areas in Padang city) shows that liquefaction occurred with a low-frequency range (0.20-0.39 Hz), indicating a soft soil type (long period >1 s). The limitation of this study is that it is assumed that the earthquake event was the only giant earthquake to have occurred in this area in the last 200 years; no other earthquake was taken into account.

4. Conclusion

This comprehensive study on liquefaction potential in Padang City integrates multiple assessment methodologies to establish reliable natural frequency thresholds for liquefaction risk evaluation. Our analysis, conducted at 54 identical sites across the city, demonstrates significant spatial and depth-dependent variations in liquefaction susceptibility. At shallow depths (0-4 m), nearly the entire study area exhibits vulnerability to liquefaction, with coastal regions showing particularly high susceptibility. The liquefaction potential generally decreases with increasing depth, confirming the stratified nature of this geotechnical hazard. Through the systematic correlation of data from field surveys documenting the 2009 Padang earthquake liquefaction events, detailed soil investigations (CPT and SPT), and microtremor single observations, we have established that locations with natural frequencies exceeding 0.40 Hz remain safe from liquefaction, while sites with frequencies within the 0.20-0.39 Hz range demonstrate significant liquefaction potential. This natural frequency threshold provides engineers, urban planners, and disaster management authorities with a practical parameter for preliminary liquefaction risk assessment that can be efficiently measured in the field. The integration of multiple assessment methods at identical sites enhances the reliability of our findings, offering a more holistic approach to liquefaction hazard mitigation. However, to further validate and refine these thresholds, future research should incorporate data from multiple seismic events that have triggered liquefaction in the region, rather than relying exclusively on the 2009 earthquake data. This approach would enhance the robustness of the natural frequency-based liquefaction potential assessment methodology proposed in this study.

5. Declarations

5.1. Author Contributions

Conceptualization, R.R.P. and J.K.; methodology, R.R.P. and S.V.; validation, Z.Z. and J.K.; formal analysis, M.D.A.; investigation, R.R.P. and M.D.A.; writing—original draft preparation, R.R.P.; writing—review and editing, J.K. and S.V.; visualization, M.D.A.; supervision, R.R.P. and J.K. All authors have read and agreed to the published version of the manuscript.

5.2. Data Availability Statement

The data presented in this study are available in the article.

5.3. Funding and Acknowledgements

We would like to thank Professor Yusuke Ono from Tottori University, Japan, for contributing to the review and ideas for our conducted research. We would also like to thank the Universitas Negeri Padang, who supported the research funding for the international research collaboration schema and fundamental research scheme year 2022-2024.

5.4. Conflicts of Interest

The authors declare no conflict of interest.

6. References

[1] Daniell, J. E., Khazai, B., Wenzel, F., & Vervaeck, A. (2011). The CATDAT damaging earthquakes database. Natural Hazards and Earth System Science, 11(8), 2235–2251. doi:10.5194/nhess-11-2235-2011.

[2] Putra, R. R., Kiyono, J., & Furukawa, A. (2014). Vulnerability assessment of non-engineered houses based on damage data of the 2009 padang earthquake in Padang city, Indonesia. International Journal of GEOMATE, 7(2), 1076–1083. doi:10.21660/2014.14.140714.

[3] Putra, R. R., Ono, Y., Syah, N., & Cantika, A. A. (2021). Seismic performance evaluation of existing building in earthquake prone area based on seismic index and seismic demand method. Civil Engineering and Architecture, 9(4), 1237–1245. doi:10.13189/cea.2021.090425.

[4] Iskandar, A., Rifa'i, A., & Hardiyatmo, H. C. (2024). the Influence of Earthquake Significant Duration on Liquefaction Potential in Area Pasar Raya Padang. International Journal of GEOMATE, 27(123), 100–107. doi:10.21660/2024.123.4687.

[5] Hakam, A., Adji, B. M., Junaidi, & Risayanti, B. M. (2018). Liquefaction analysis of abrasion protection structure in Padang. MATEC Web of Conferences, 229, 1018. doi:10.1051/matecconf/201822901018.

[6] Tohari, A., Sugianti, K., & Soebowo, E. (2011). Liquefaction Potential at Padang City: a Comparison of Predicted and Observed Liquefactions during the 2009 Padang Earthquake. Journal of Geology and Mining Research, 21(1), 7. doi:10.14203/risetgeotam2011.v21.42.

[7] Rezaei, S., & Choobbasti, A. J. (2014). Liquefaction assessment using microtremor measurement, conventional method and artificial neural network (Case study: Babol, Iran). Frontiers of Structural and Civil Engineering, 8(3), 292–307. doi:10.1007/s11709-014-0256-8.

[8] Unjoh, S., Kaneko, M., Kataoka, S., Nagaya, K., & Matsuoka, K. (2012). Effect of earthquake ground motions on soil liquefaction. Soils and Foundations, 52(5), 830–841. doi:10.1016/j.sandf.2012.11.006.

[9] Ghani, S., Kumari, S., & Bardhan, A. (2021). A novel liquefaction study for fine-grained soil using PCA-based hybrid soft computing models. Sadhana - Academy Proceedings in Engineering Sciences, 46(3), 113. doi:10.1007/s12046-021-01640-1.

[10] Muhammad, N. B., Namdar, A., & Zakaria, I. Bin. (2013). Liquefaction mechanisms and mitigation-a review. Research Journal of Applied Sciences, Engineering and Technology, 5(2), 574–567. doi:10.19026/rjaset.5.4992.

[11] Wei, X., Zhuang, Y., Yang, J., & Zhang, L. (2024). Excess pore pressure generation in silty sands subjected to cyclic triaxial loading. Japanese Geotechnical Society Special Publication, 10(17), 552-557.

[12] Jalil, A., Fathani, T. F., Satyarno, I., & Wilopo, W. (2021). Liquefaction in Palu: the cause of massive mudflows. Geoenvironmental Disasters, 8(1), 21. doi:10.1186/s40677-021-00194-y.

[13] Bozzoni, F., Bonì, R., Conca, D., Lai, C. G., Zuccolo, E., & Meisina, C. (2021). Megazonation of earthquake-induced soil liquefaction hazard in continental Europe. Bulletin of Earthquake Engineering, 19(10), 4059–4082. doi:10.1007/s10518-020-01008-6.

[14] Pokhrel, R. M., Gilder, C. E. L., Vardanega, P. J., De Luca, F., De Risi, R., Werner, M. J., & Sextos, A. (2022). Liquefaction potential for the Kathmandu Valley, Nepal: a sensitivity study. Bulletin of Earthquake Engineering, 20(1), 25–51. doi:10.1007/s10518-021-01198-7.

[15] Sonmezer, Y. B. (2019). Energy-based evaluation of liquefaction potential of uniform sands. Geomechanics and Engineering, 17(2), 145–156. doi:10.12989/gae.2019.17.2.145.

[16] Bensoula, M., Bousmaha, M., & Missoum, H. (2022). Relative density influence on the liquefaction potential of sand with fines. Revista de La Construccion, 21(3), 692–702. doi:10.7764/RDLC.21.3.692.

[17] Bray, J. D., & Dashti, S. (2014). Liquefaction-induced building movements. Bulletin of Earthquake Engineering, 12(3), 1129–1156. doi:10.1007/s10518-014-9619-8.

[18] Lai, C. G., Bozzoni, F., Conca, D., Famà, A., Özcebe, A. G., Zuccolo, E., Meisina, C., Bonì, R., Bordoni, M., Cosentini, R. M., Martelli, L., Poggi, V., Viana da Fonseca, A., Ferreira, C., Rios, S., Cordeiro, D., Ramos, C., Molina-Gómez, F., Coelho, C., … Kelesoglu, M. K. (2021). Technical guidelines for the assessment of earthquake induced liquefaction hazard at urban scale. Bulletin of Earthquake Engineering, 19(10), 4013–4057. doi:10.1007/s10518-020-00951-8.

[19] Ng, C. W. W., Crous, P. A., Zhang, M., & Shakeel, M. (2022). Static liquefaction mechanisms in loose sand fill slopes. Computers and Geotechnics, 141, 104525. doi:10.1016/j.compgeo.2021.104525.

[20] Boulanger, R. W., & Idriss, I. M. (2008). Closure to "Liquefaction Susceptibility Criteria for Silts and Clays" by Ross W. Boulanger and I. M. Idriss. Journal of Geotechnical and Geoenvironmental Engineering, 134(7), 1027–1028. doi:10.1061/(asce)1090-0241(2008)134:7(1027).

[21] Seed, H. B., & Idriss, I. M. (1971). Simplified Procedure for Evaluating Soil Liquefaction Potential. Journal of the Soil Mechanics and Foundations Division, 97(9), 1249–1273. doi:10.1061/jsfeaq.0001662.

[22] Tsai, C. C., & Li, P. C. (2024). Quantifying near-fault motion effects on soil liquefaction through effective stress site response analysis. Soil Dynamics and Earthquake Engineering, 183, 108779. doi:10.1016/j.soildyn.2024.108779.

[23] Yıldız, Ö., Zeybek, A., & Sönmezer, Y. B. (2024). Investigation of the earthquake-induced liquefaction and seismic amplifications after Pazarcık (Mw 7.7) and Elbistan (Mw 7.6) earthquakes. Environmental Earth Sciences, 83(21). doi:10.1007/s12665-024-11921-7.

[24] Putra, R. R. (2017). Estimation of VS30 based on soil investigation by using microtremor observation in Padang, Indonesia. International Journal of GEOMATE, 13(38), 135–140. doi:10.21660/2017.38.tvet030.

[25] Pramono, P., Widjaja, B., Herina, S., Lestari, A. S., Lim, A., Rustiani, S., ... & Hapsari, V. (2014). Geotechnical Study of Infrastructure for Padang City Facing the Threat of Earthquakes and Tsunamis. Research Report - Engineering Science, 1-58. (In Indonesian).

[26] Basu, D., Montgomery, J., & Stuedlein, A. W. (2022). Observations and challenges in simulating post-liquefaction settlements from centrifuge and shake table tests. Soil Dynamics and Earthquake Engineering, 153. doi:10.1016/j.soildyn.2021.107089.

[27] Sukkarak, R., Tanapalungkorn, W., Likitlersuang, S., & Ueda, K. (2021). Liquefaction analysis of sandy soil during strong earthquake in Northern Thailand. Soils and Foundations, 61(5), 1302–1318. doi:10.1016/j.sandf.2021.07.003.

[28] Wang, J., Ge, X., Sun, J., Liu, Y., Shang, Z., Wang, Z., & Tian, M. (2023). Dynamic response analysis of liquefiable ground due to sinusoidal waves of different frequencies of shield construction. Earthquake Engineering and Engineering Vibration, 22(3), 637–646. doi:10.1007/s11803-023-2192-x.

[29] Widiyantoro, S., Gunawan, E., Muhari, A., Rawlinson, N., Mori, J., Hanifa, N. R., ... & Putra, H. E. (2020). Implications for megathrust earthquakes and tsunamis from seismic gaps south of Java Indonesia. Scientific Reports, 10(1), 15274. doi:10.1038/s41598-020-72142-z.

[30] Putra, R. R. (2020). Damage investigation and re-analysis of damaged building affected by the ground motion of the 2009 Padang earthquake. International Journal of GEOMATE, 18(66), 163–170. doi:10.21660/2020.66.Icee2nd.

[31] Boumpoulis, V., Depountis, N., Pelekis, P., & Sabatakakis, N. (2021). SPT and CPT application for liquefaction evaluation in Greece. Arabian Journal of Geosciences, 14(16), 1–15. doi:10.1007/s12517-021-08103-1.

[32] Youd, T. L., & Idriss, I. M. (1997). Proceeding of the NCEER workshop on evaluation of liquefaction resistance of soils. Technical Report NCEER-97-0022.

[33] Sonmez, H., & Gokceoglu, C. (2005). A liquefaction severity index suggested for engineering practice. Environmental Geology, 48(1), 81–91. doi:10.1007/s00254-005-1263-9.

[34] Robertson, P. K., & Wride, C. E. (1998). Evaluating cyclic liquefaction potential using the cone penetration test. Canadian Geotechnical Journal, 35(3), 442–459. doi:10.1139/t98-017.

[35] Nakamura, Y. (1989). A method for dynamic characteristics estimation of subsurface using microtremor on the ground surface. Railway Technical Research Institute, Quarterly Reports, 30(1), 25-33.

[36] Nakamura, Y. (2000). Clear identification of fundamental idea of Nakamura's technique and its applications. Proceedings of the 12th world conference on earthquake engineering, 30 January-4 February 2000, Auckland, New Zealand.

[37] Li, C. Y., Wu, J. H., Lee, D. H., & Chen, K. Y. (2021). Investigating the Ground Characteristics Using HVSR Curves with Microtremor Measurements: The Urban Area in Tainan. Journal of the Chinese Institute of Civil and Hydraulic Engineering, 33(2), 125–138. doi:10.6652/JoCICHE.202104_33(2).0005.

[38] Rezaei, S., & Choobbasti, A. J. (2017). Application of the microtremor measurements to a site effect study. Earthquake Science, 30(3), 157–164. doi:10.1007/s11589-017-0187-2.

[39] Bonnefoy-Claudet, S., Cotton, F., & Bard, P. Y. (2006). The nature of noise wavefield and its applications for site effects studies. A literature review. Earth-Science Reviews, 79(3–4), 205–227. doi:10.1016/j.earscirev.2006.07.004.

[40] SESAME. (2004). Guidelines for the Implementation of the H/V Spectral Ratio Technique on Ambient Vibrations: Measurements, Processing and Interpretation. SESAME European Research Project WP12, 1-62.

[41] Kennedy, C. (2024). Shear Wave Velocity as a Measure of the Dynamic Properties of Confined Silty Soil. Research Square (Preprint), 1-12. doi:10.21203/rs.3.rs-4337341/v1.

[42] Karagianni, E. E., Papazachos, C. B., Panagiotopoulos, D. G., Suhadolc, P., Vuan, A., & Panza, G. F. (2004). Shear velocity structure in the Aegean area obtained by inversion of Rayleigh waves. Geophysical Journal International, 160(1), 127–143. doi:10.1111/j.1365-246x.2005.02354.x.

[43] Torsvik, T. H., Rousse, S., Labails, C., & Smethurst, M. A. (2009). A new scheme for the opening of the South Atlantic Ocean and the dissection of an Aptian salt basin. Geophysical Journal International, 177(3), 1315-1333. doi:10.1111/j.1365-246X.2009.04137.x.

[44] Liang, D., Gan, F., Zhang, W., & Jia, L. (2018). The application of HVSR method in detecting sediment thickness in karst collapse area of Pearl River Delta, China. Environmental earth sciences, 77(6), 259. doi:10.1007/s12665-018-7439-x.

[45] Nakamura, Y. (1997). Seismic vulnerability indices for ground and structures using microtremor. World Congress on Railway Research, November 1997, Florence, Italy.

[46] Xu, C., Yue, C., Du, X., Liang, K., Wang, B., & Chen, G. (2025). Experimental study on the influence of cyclic loading frequency on liquefaction characteristics of saturated sand. Géotechnique, 75(4), 501–514. doi:10.1680/jgeot.21.00384.

[47] Choobbasti, A. J., Naghizadehrokni, M., & Rezaei, S. (2015). Liquefaction assessment by microtremor measurements in Babol city. In Fifth International Conference on Geotechnique, Construction Materials and Environment, 16-18 November, 2015, Osaka, Japan.

[48] Yuan, X., Sun, R., Chen, L., & Tang, F. (2010). A method for detecting site liquefaction by seismic records. Soil Dynamics and Earthquake Engineering, 30(4), 270–279. doi:10.1016/j.soildyn.2009.12.003.

[49] Zhu, Z., Zhang, F., Peng, Q., Dupla, J.-C., Canou, J., Cumunel, G., & Foerster, E. (2021). Effect of the loading frequency on the sand liquefaction behaviour in cyclic triaxial tests. Soil Dynamics and Earthquake Engineering, 147, 106779. doi:10.1016/j.soildyn.2021.106779.

[50] Sitharam, T. G., GovindaRaju, L., & Sridharan, A. (2004). Dynamic properties and liquefaction potential of soils. Current Science, 87(10), 1370–1378.

[51] Chang, N.-Y., Hsieh, N.-P., Samuelson, D. L., & Horita, M. (1982). Effect of Frequency on Liquefaction Potential of Saturated Monterey No. O Sand. Computational Methods and Experimental Measurements, 433–446, Springer, Berlin, Germany. doi:10.1007/978-3-662-11353-0_34.

[52] Jahankhah, H., & Farashahi, P. F. (2017). The effect of foundation embedment on net horizontal foundation input motion: the case of strip foundation with incomplete contact to nearby medium. Soil Dynamics and Earthquake Engineering, 96, 35-48. doi:10.1016/j.soildyn.2017.02.015.

[53] Mehrzad, B., Jafarian, Y., Lee, C. J., & Haddad, A. H. (2018). Centrifuge study into the effect of liquefaction extent on permanent settlement and seismic response of shallow foundations. Soils and foundations, 58(1), 228-240. doi:10.1016/j.sandf.2017.12.006.